



Laser ablation inductively coupled plasma mass spectrometry analysis of isotopically heterogeneous uranium materials

Zsolt Varga¹ · Maria Wallenius¹ · Adrian Nicholl¹ · Klaus Mayer¹

Received: 23 June 2022 / Accepted: 6 August 2022 / Published online: 1 September 2022
© The Author(s) 2022

Abstract

A reliable and accurate laser ablation multi-collector inductively coupled plasma mass spectrometry (LA-MC-ICP-MS) method was developed for analysis of inhomogeneous samples containing uranium particles or aggregates of various enrichments. For the method development, a mixed solid standard was prepared using 1% and 3% ²³⁵U enriched certified reference materials. After screening and localization of the particles of interest, the U isotopic composition was analysed for a 5- μ m sample spot determining accurately and precisely the various constituents. Besides the LA-MC-ICP-MS, the standard was also measured by large-geometry secondary ion mass spectrometry (LG-SIMS) for additional verification.

Keywords Nuclear forensics · Inhomogeneous samples · Uranium · Inductively coupled plasma mass spectrometry · Laser ablation

Introduction

Nuclear forensic methods aim at providing hints on the intended use, origin, production time and history of nuclear and other radioactive materials [1–5]. The scientific measurement results obtained on the evidence enable drawing nuclear forensic conclusions and may serve law enforcement as investigative leads. Several characteristic parameters (usually referred to as “signatures”) can be used to re-establish the material history, such as physical dimensions of the material, isotopic composition of U and Pu, impurities or production date [1, 2, 4], hence to link the material in question to a production process or even to a specific facility. Moreover, traditional forensic evidence associated with the material may help to identify individuals who handled it [3, 4, 6].

Besides the commonly measured bulk characteristics of the investigated material, the real-world items with inhomogeneity bear information at microscopic scale. These inhomogeneities (e.g. depositions or layers with different elemental or isotopic composition, often assorted with non-radioactive materials) can provide potentially additional

information on the material and its production history other than the conventionally applied techniques. Confiscated radioactive samples, e.g. contaminated scrap metals or U pellets are typical examples, where inhomogeneity has been encountered [7–10]. The importance of examining the inhomogeneity of the sample and the currently available measurement capabilities were underlined during the Collaborative Materials Exercise (CMX-5) organized by the Nuclear Forensics International Technical Working Group (ITWG) in 2017 [7]. A study by Jovanovic et al. compared the use of different analytical methods to characterize the inhomogeneous uranium isotopic compositions of uranium pellets, which were manufactured with distinct production routes and levels of inhomogeneity, but had identical bulk uranium isotopic compositions [8]. Only few analytical techniques are capable of measuring the isotopic composition with spatial resolution (down to micron scale) directly, such as secondary ion mass spectrometry (SIMS) [9–12], and laser ablation (LA) coupled to an inductively coupled plasma mass spectrometry (ICP-MS) [13, 14].

The aim of this study was to develop a reliable method by LA-MC-ICP-MS for spatially resolved U isotope measurements of solid samples down to μ m scale. As the results of such measurements form the basis for important decisions by the investigative authorities, the method requires exhaustive validation for defensible conclusions. The analytical settings and instrumental conditions (e.g. ablation cell type, laser

✉ Zsolt Varga
Zsolt.Varga@ec.europa.eu

¹ European Commission, Joint Research Centre (JRC), Karlsruhe, Germany

beam diameter or scan speed) may fundamentally modify the elemental concentration and can change the obtained pattern [15, 16], this alteration is also expected for isotope ratios. Thus, the instrumental parameters need to be optimized, potential effects need to be corrected for and finally a careful validation of the method is required. To this end, a synthetic mixture was prepared by blending powders of two certified reference materials (CRMs) with 1% and 3% ^{235}U enrichments. As only a transient signal can be obtained by laser ablation ICP-MS, the precision of the measured isotope ratio is limited by counting statistics and by time dependent variation of the measured ion currents. Therefore, additional effort was invested to develop a method with improved precision.

Experimental

Materials and instrumentation

The measured U samples, SRM U-010 and SRM U-030, are standard reference materials in form of U_3O_8 purchased from National Bureau of Standards (NBS, Washington DC, USA), presently distributed by New Brunswick Laboratory (NBL, Argonne, IL, USA) [17, 18]. The certified $^{234}\text{U}/^{238}\text{U}$ and $^{235}\text{U}/^{238}\text{U}$ amount ratios of SRM U-010 are $5.47(5) \times 10^{-5}$ and $1.0140(10) \times 10^{-2}$, respectively [17], while the certified $^{234}\text{U}/^{238}\text{U}$ and $^{235}\text{U}/^{238}\text{U}$ amount ratios of SRM U-030 are $1.961(10) \times 10^{-4}$ and $3.1430(31) \times 10^{-2}$, respectively [18]. The particles were different in size, ranging from sub-micrometer to hundreds of micrometer.

A NuPlasmaTM (NU Instruments, Wrexham, United Kingdom) double-focusing multi-collector inductively coupled plasma mass spectrometer (MC-ICP-MS), equipped with 11 Faraday detectors and 3 discrete dynode electrode multipliers was used for the U isotopic measurements. The MC-ICP-MS was connected to a NWR-213 laser ablation unit (ESI, Huntingdon, UK) for solid samples. The instrument was operated in low mass resolution mode ($R = 300$). The MC-ICP-MS was optimised daily (torch position, gas flows, voltages) using a 30 ng g^{-1} multi-elemental solution (Inorganic Ventures, Christiansburg, USA). The optimisation aimed at achieving highest sensitivity and stability of the acquired U signal. The sensitivity was about 6 V for $^{238}\text{U}^+$. The LA system was equipped with a two-volume cell (called TV2 cell in this design) to eliminate cross-contamination of other samples and within the LA chamber. Before the actual LA analysis, the sample was pre-ablated (i.e. the surface was cleaned and smoothed) with the laser beam (diameter: $50 \mu\text{m}$, scan rate: $50 \mu\text{m s}^{-1}$). If the sample surface contains relevant information, the pre-ablation may not be necessary. Here, this was used to avoid any contamination from the laboratory press. The raw data were corrected for the gas

blank. Mass bias correction and ion counter gains were calculated using a NBS U-020 CRM pellet that was measured before the analysis of each sample. Further details of the instrumentation and optimization can be found elsewhere [19]. Detailed instrumental settings and data acquisition parameters are given in Table 1.

The depth of the laser ablation crater is $< 100 \text{ nm}$ with the applied low fluence (corresponds to $< 2 \mu\text{m}^3$ in volume for a single laser shot with $5 \mu\text{m}$ diameter) [19]. Thus, for a $100 \mu\text{m}$ line with $5 \mu\text{m}$ laser diameter $< 2 \text{ ng}$ material is required for the analysis. The laser ablation diameter can go down to nominally $2 \mu\text{m}$, so this is the smallest spatial resolution which can be detected from the LA point of view.

The LG-SIMS measurements were performed on a CAMECA IMS 1280-HR, a large geometry double focusing magnetic sector secondary ion mass spectrometer (LG-SIMS). The search for U particles was done in raster imaging mode using $500 \mu\text{m} \times 500 \mu\text{m}$ areas over the whole sample planchet. The microbeam measurements were performed on individual particles over a smaller area ($10 \mu\text{m} \times 10 \mu\text{m}$). Further details can be found elsewhere [20].

The U samples were observed also by scanning electron microscopy (SEM) using a Vega Tescan instrument (TS5130LSH, Czech Republic) to investigate the particle morphology. The SEM was operated at 20 kV with a typical emission current of $50 \mu\text{A}$. Before the analysis, the samples were coated with a thin carbon layer to avoid charging effects on the surface.

Preparation of U standards

The solid U standards were used as such, without further manipulation (i.e. no dissolution or grinding) to preserve their original characteristics, in particular the shape of the particles, as much as possible. Besides measuring the SRM U-010 and U-030 standards alone, an approx. 1:1 mixture of the CRMs was prepared. For this, the U-010 and U-030 standards were mixed in a plastic vial and homogenised by gentle shaking for 10 min. This procedure was performed in a careful manner to avoid deterioration of the particles. The powder samples were then pressed into pellets with an X-PRESS hydraulic laboratory press (Spex Industries, Metuchen, USA) using 2 tons for 8 min. The pellets' diameter was 5 mm and the height was approximately 1 mm. In order to avoid contamination of the hydraulic press and to evade cross-contamination, pre-cleaned plastic covers were used on both sides of the pressed pellet. No binder was used. By visual inspection and scanning electron microscopy, large grains (up to $200 \mu\text{m}$) with smaller particles on the surface (around $1 \mu\text{m}$) were observed (Fig. 1).

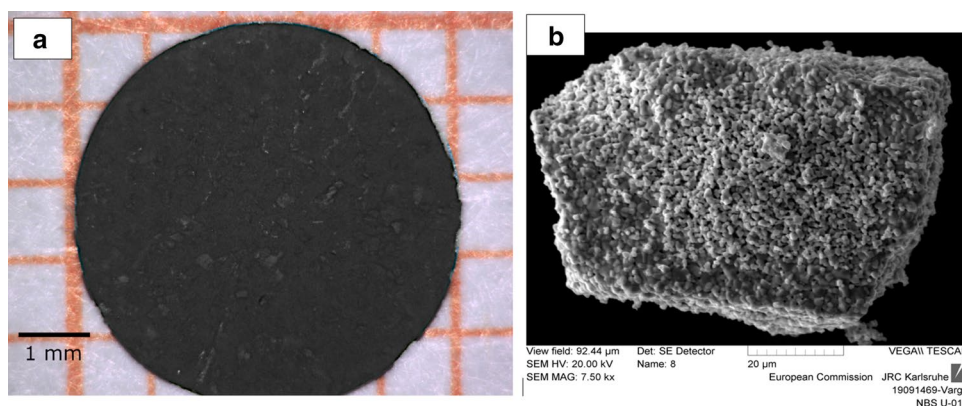
The individual U standards and the mixture were also measured by LG-SIMS. Even though the LG-SIMS cannot validate the LA-MC-ICP-MS results (the measured samples

Table 1 MC-ICP-MS and LA operating parameters

MC-ICP-MS instrument settings	
Forward power (W)	1300
Cooling gas flow rate (L min ⁻¹)	14.0
Auxiliary gas flow rate (L min ⁻¹)	0.98–1.05
Nebulizer gas flow rate (L min ⁻¹)	0.90–0.98
Data acquisition	
Mass resolution	~300
Number of spectra acquired	~2700
Magnet delay between blocks (s)	2
Scan type	Static multi-collection
Time of data point acquisition (ms)	200
Cup configuration*	IC0: ²³⁶ U, IC1: ²³⁴ U, L1: ²³⁵ U, L3: ²³⁸ U
Laser ablation conditions	
LA-system	NWR-213 equipped with TV2 cell
Laser type	Nd:YAG
Ablation gas	He
Ablation gas flow (mL min ⁻¹)	50
Pulse duration (ns)	2.1
Wavelength (nm)	213
Repetition rate (Hz)	5–10
Fluence (J cm ⁻²)	0.2–1.9

*L1 and L3 denote Faraday detectors; IC0 and IC1 denote discrete dynode electron multipliers operated in pulse counting mode. IC0 is also equipped with a retardation filter for improving abundance sensitivity

Fig. 1 Optical microscopy image of the obtained pressed pellet for LA measurements (a) and SEM image of an U particle of SRM U-010 (b)



are in different forms), it can verify the LA findings. For the LG-SIMS measurement, the materials were analysed in the native powder form, i.e. a very small amounts of the U samples (in µg range) were placed on cotton swipes. The particles from the swipes were transferred onto a planchet (SPI Pyrolytic Graphite Planchet, 25.4×3.2 mm) using a vacuum impactor technique [21].

Results and discussion

LA-MC-ICP-MS characterization of the mixture

The mixture of SRM U-010 and U-030 was analysed by LA-MC-ICP-MS to investigate its isotopic properties.

Before the actual measurement, pre-ablation was performed on the sample with the same laser conditions, but only with larger laser beam size in order to clean the surface and decrease the surface roughness. Besides the observable large grains by optical microscopy, the LA analysis revealed isotope inhomogeneity in the sample. Several chromatograms (i.e. isotope ratios vs. ablation time) were obtained and values between 1% and 3% ^{235}U enrichment depending on if single particles or particle agglomerations were measured. Subject to the starting point and the position of the ablation, the measured ^{235}U enrichment values can be anything between 1% and 3%. For the sake of easier understanding, a representative chromatogram was chosen from the measured set as an example (Fig. 2). In the line scan, large and relatively homogeneous agglomerates up to 200 μm can be identified, while the sharp variations (spikes) belong to smaller particles.

The mixture was also measured by LG-SIMS: an automated screening measurement found 2200 uranium particles. More precise microbeam measurements were performed on 30 individual particles and showed two distinct ^{235}U enrichment populations of about 1.01% and 3.06% (Fig. 3). This finding agreed well with the certified values and confirmed the validity of the obtained LA-MC-ICP-MS results.

Figure 4 shows the measurement of the individual SRM U-010 and U-030 standards by LG-SIMS. It has to be noted that two slightly different, but statistically significant distinct groups of ^{235}U enrichment for the SRM U-010 material were visible: one is centred around 0.97%, another one is 1.01%; while the SRM U-030 is more isotopically homogeneous at particle level. One has to note that these reference materials are intended for bulk measurements and not for the particle-level U isotopic measurement. The NBL Program Office recommends the use of 1 mg or more of this material as stated in the certificates of the CRMs [17]. However,

Fig. 2 Line scan of the mixed sample, 80 μm line (conditions: laser beam size: 3 μm , scan speed: 1 $\mu\text{m s}^{-1}$, repetition rate: 10 Hz)

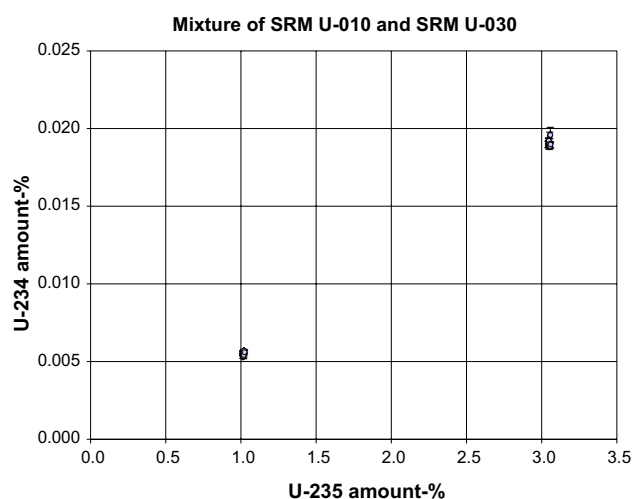
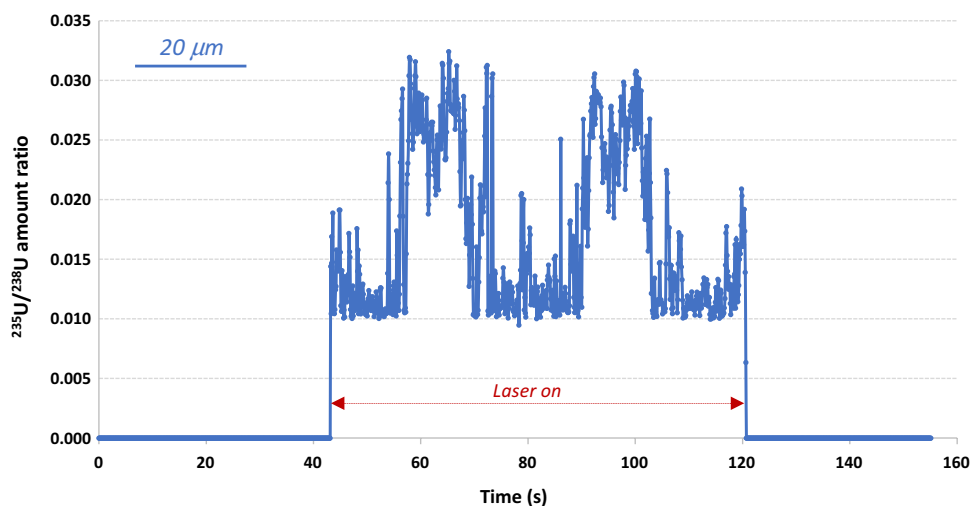


Fig. 3 LG-SIMS measurement of the SRM U-010 and U-030 mixture

as the ^{235}U abundance spread is lower than the uncertainty of LA-MC-ICP-MS analysis features, it will not affect the precision of the present study.

Effects of laser ablation parameters

As the instrumental parameters have a vital effect on the measured signal and thus on the final results, they have to be checked and optimized before the analysis. This effect was demonstrated in the case of elemental concentration [15]. The main factors affecting the result (besides the other parameters defined by the instrumental setting) are found to be the laser beam diameter, scan speed and repetition rate.

In order to investigate the effect of the laser beam diameter, a pre-ablation was performed on the sample to remove the surface contamination and to have an identical surface. The pre-ablation width was 50 μm , which is much larger

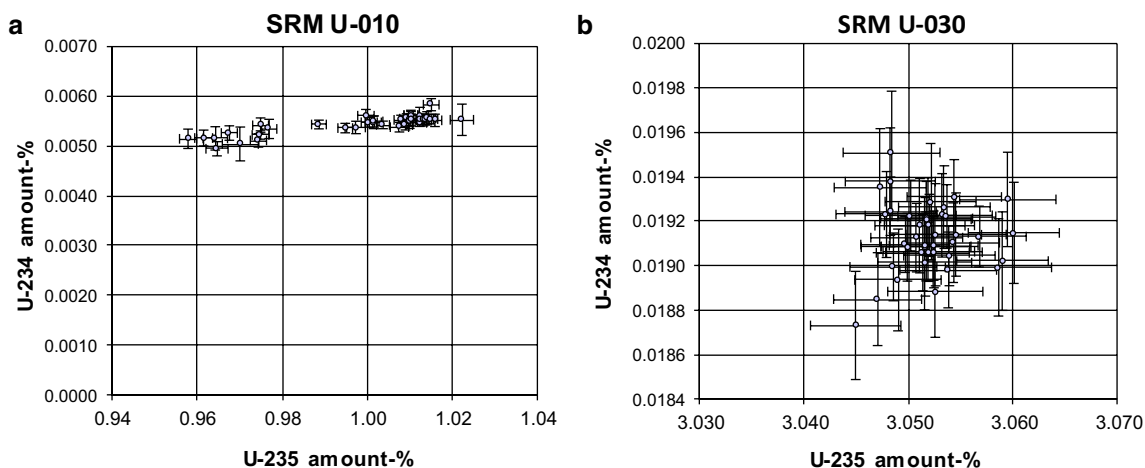


Fig. 4 LG-SIMS measurement of the individual particles of SRM U-010 **a** and U-030 **b** CRMs

than the maximum of the applied laser beam diameters. To compare the various laser beam diameters, the ablation was performed in the same line successively with a laser beam diameter of 3, 8 and 20 μm , respectively. After this ablation series, the analyses were repeated once more on the same line to make sure that the sample ablation did not change the observed pattern. The repeated measurements with the same laser beam diameter resulted in identical values within the measurement uncertainty. In order to demonstrate the LA effect on the obtained signal, a specific area was chosen, which contained a distinctive pattern: two particles of SRM U-030 embedded in larger amount of SRM U-010.

The obtained LA scans on the same line, using different beam diameters together with the respective histograms are shown in Fig. 5. The isotopic pattern is recognizable in all cases; however, there are clear differences in the measured signals using different beam sizes. The sharp peaks (spikes), belonging to the small particles, are observed only with the smallest laser beam diameter (i.e. less than the particle diameter). Thus, by applying a smaller laser beam diameter more sharp peaks and fine structures are visible. Moreover, when smaller laser beam diameter is used, the measured $^{235}\text{U}/^{238}\text{U}$ isotope ratios are closer to the certified isotope ratios of the two starting materials. It has to be emphasized that a too big laser beam diameter will yield to an averaging effect as several adjacent particles are measured together. In other words, spatial information is lost and, by consequence, inaccurate isotope ratio results are obtained resulting in misleading interpretation. The reason for this is that if the laser beam diameter is higher than the later size of the particle, one will get the mix (average) of this ablated particle with the adjacent environment. This is reflected in particular in the histogram in Fig. 4 C, where the $^{235}\text{U}/^{238}\text{U}$ amount ratios of the constituting CRMs are not observable due to the too high laser beam diameter. Moreover, use of a

smaller beam diameter is vital for 2D-imaging, as the fine structure of the surface can only be acquired with a small diameter, otherwise only a blurred image is obtained [15]. A disadvantage, however, is that in this case a smaller area of the sample can be covered compared to larger laser beam diameters and the areas of interest may remain undetected. Therefore, it is advisable to screen other areas of the sample as well to compensate for this. As the typical LA analysis time is only a few minutes, it is doable to scan several areas to obtain comprehensive information.

The sample was also analyzed with different scan speeds (1, 5, 10 $\mu\text{m s}^{-1}$) keeping the laser beam size constant (3 μm). Higher scan speed resulted in the same effect similar to larger laser beams: If too fast scanning speed is used, significant areas are measured together with the surrounding areas resulting an averaging with the adjacent positions. Moreover, the measured isotope ratios can also be erroneous depending on the particle size similar to the laser beam diameter. In this case, the overall measurement time is also affected: more analysis time is needed at lower scan speed. The repetition rate should be adjusted to the laser beam diameter and scan speed not to have non-measured (missed) points [15].

To sum up, both the laser beam diameter and scan speed have a substantial impact on the accuracy and required analysis time. Therefore, it is advisable to analyze and scan different areas of the sample using different LA beam diameter and scan speed.

Precise measurement of an area of interest

The biggest challenge in the precise measurement of a LA signal is the transient (time-dependent) behavior [21]. In this case, only a short signal is obtained as a function of time. The resulting isotope ratios have poor precision,

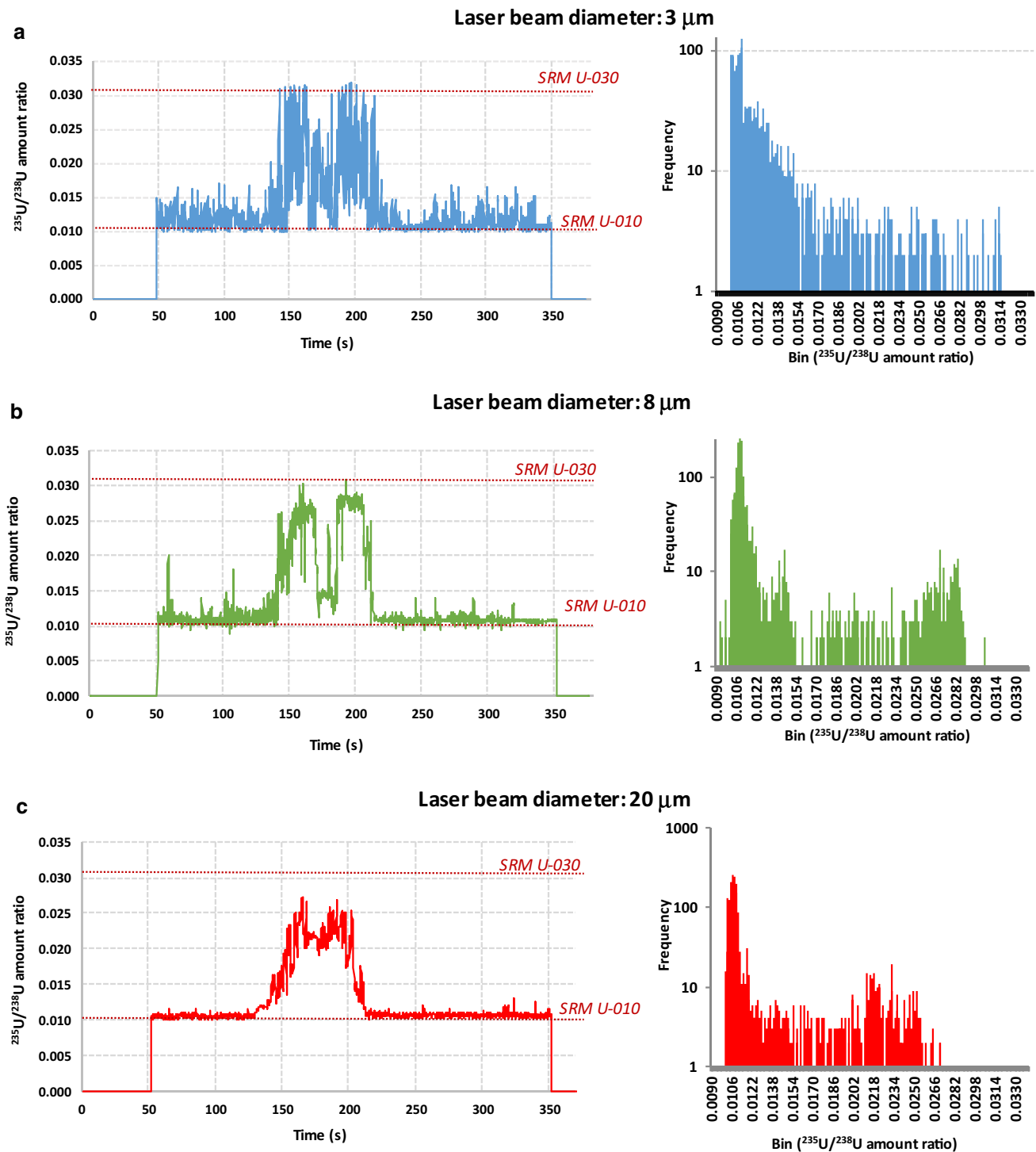


Fig. 5 Measured LA-MC-ICP-MS chromatograms and the respective histograms (note the fixed x range for the histograms) measured with different laser diameter (scan speed was fixed to $1 \mu\text{m s}^{-1}$) on the

same line. Laser ablation diameter A: 3 μm , B: 8 μm , and C: 20 μm . The $^{235}\text{U}/^{238}\text{U}$ amount ratios of the constituting U reference materials are also indicated

as only a few data points are acquired for a given position. A possible solution to this issue is a two-step process, where the first step is to screen the area of interest (localization) using line scan. In a second step, when the

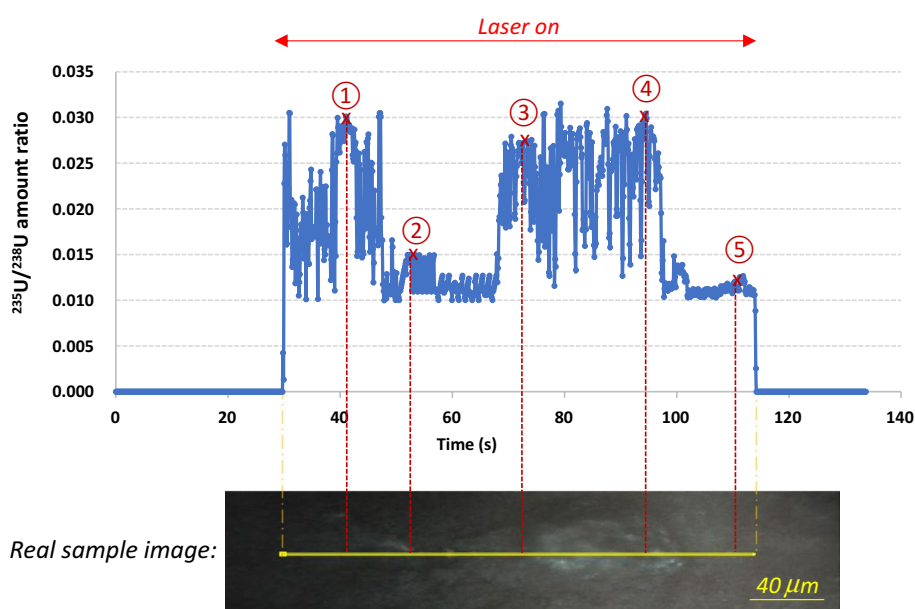
point-of-interest (POI), e.g. higher ^{235}U abundance has been found and selected, a spot analysis is performed on that small area resulting in a more precise measurement

results. In practice, this method can be realized in the following way:

1. Pre-ablation (sputtering) of the area with larger LA beam diameter before the measurements.
2. Screening of the investigated surface using a line scan keeping the y coordinate constant. The coordinates of the starting and end points are marked ((x_{start}, y) and (x_{end}, y) , respectively). The speed of the line scan is known and should be kept constant.
3. The U isotope ratio as a function of time (chromatogram) is measured by ICP-MS. A number of spectra are acquired during the measurement along the screened line.
4. As the end points of the chromatogram are sharp, the (x_{start}, y) and (x_{end}, y) points of the real sample can be assigned to the chromatogram (Fig. 6). Knowing the constant speed of the laser ablation, the position of the measured signal in the chromatogram can be assigned to sample positions (i.e. the measured spectrum number at a certain position can be assigned to (x, y) of the sample). Then, using the chromatogram the measurable positions (POIs) can be selected.
5. The sample on the laser ablation stage can be moved to the required (x_{POI}, y) position to perform the precise spot measurement with fixed stage position.

For instance, if 400 spectra are taken for a 200 μm line at constant ablation speed, the 100th spectrum belongs to the position 50 μm from the start of the LA signal. Then the LA stage can be moved to this (x_{POI}, y) position to execute the fixed, precise isotope ratio measurement.

Fig. 6 Image of the real sample (down) together with the respective chromatogram obtained by LA-MC-ICP-MS. The selected POIs and real positions are marked



An example is shown in Fig. 6. Firstly, a line scan was performed on the pre-ablated surface (pre-ablation conditions: scan speed of 50 $\mu\text{m s}^{-1}$ and laser diameter of 50 μm) to screen the sample and localize the POIs. The conditions for the screening (line scan): scan speed of 1 $\mu\text{m s}^{-1}$ with the laser diameter of 3 μm . When the POIs were selected based on the chromatogram and the correlation of the spectrum number vs. the y position was calculated, the laser stage was moved to the exact (x, y) position to perform a spot measurement. The overall procedure (screening and precise measurement) is somewhat similar to SIMS particle localization [20].

Table 2 shows the measured spot results of the selected POIs. Three replicate measurements were performed on the selected position using a 3 μm laser beam diameter. The major $^{235}\text{U}/^{238}\text{U}$ amount ratio can be determined with a relative uncertainty of 0.76–1.8%, while the minor $^{234}\text{U}/^{238}\text{U}$ can be measured with a relative uncertainty of 5.7–7.1%. These uncertainty values are a factor of 3–6 higher than the U isotope ratio uncertainties of individual SRMs without mixing

Table 2 Results of the spot analysis on the selected POIs ($n=3$). The given uncertainties are expanded uncertainties with a coverage factor of $k=2$

Point-of-interest	$^{235}\text{U}/^{238}\text{U}$ amount ratio	$^{234}\text{U}/^{238}\text{U}$ amount ratio
① POI	$3.013(23) \times 10^{-2}$ (0.76%)	$1.88(11) \times 10^{-4}$ (5.9%)
② POI	$1.513(27) \times 10^{-2}$ (1.8%)	$8.78(53) \times 10^{-5}$ (6.0%)
③ POI	$2.743(22) \times 10^{-2}$ (0.80%)	$1.70(12) \times 10^{-4}$ (7.1%)
④ POI	$2.983(29) \times 10^{-2}$ (0.98%)	$1.86(12) \times 10^{-4}$ (6.5%)
⑤ POI	$1.193(18) \times 10^{-2}$ (1.5%)	$6.66(38) \times 10^{-5}$ (5.7%)

[19]. Note that the mixing and not the LA measurements result in the higher uncertainties.

In order to identify the number of constituents, a previously developed method can be used [16]. Afterwards, the precise the $^{234}\text{U}/^{238}\text{U}$ and $^{235}\text{U}/^{238}\text{U}$ of the constituents can be measured with the present technique.

Conclusions

In the present work an improved method for the accurate measurement and validation of the U isotopic composition in inhomogeneous samples was developed. Those important instrumental parameters, which can cause erroneous results, were investigated. In order to precisely measure the U isotope ratios, a two-step procedure was developed: First screening and localizing the POIs in the sample by a line scan, and then in the second step performing a precise spot measurement on the selected area. The real nuclear forensic samples were simulated with a specially prepared mixture of certified reference materials and a method comparison and verification using LG-SIMS measurement. The method can be applied in nuclear forensics, e.g. for contaminated scrap metal samples or U fuel pellets when powder blending process is suspected. Besides that, the method can be extended to 2D maps for larger areas [16] or to the measurements of other elements, e.g. rare-earth elements or other elements commonly associated with U, to improve the origin assessment of unknown illicit materials.

Acknowledgements The LG-SIMS laboratory (C. Vincent, N. Albert) is gratefully acknowledged for its indispensable contribution.

Declarations

Conflict of interests The Authors declare that there is no conflict of interest.

Open Access This article is licensed under a Creative Commons Attribution 4.0 International License, which permits use, sharing, adaptation, distribution and reproduction in any medium or format, as long as you give appropriate credit to the original author(s) and the source, provide a link to the Creative Commons licence, and indicate if changes were made. The images or other third party material in this article are included in the article's Creative Commons licence, unless indicated otherwise in a credit line to the material. If material is not included in the article's Creative Commons licence and your intended use is not permitted by statutory regulation or exceeds the permitted use, you will need to obtain permission directly from the copyright holder. To view a copy of this licence, visit <http://creativecommons.org/licenses/by/4.0/>.

References

- Mayer K, Wallenius M, Varga Z (2013) Nuclear forensic science: Correlating measurable material parameters to the history of nuclear material. *Chem Rev* 113:884–900. <https://doi.org/10.1021/cr300273f>
- Kristo MJ, Gaffney AM, Marks N et al (2016) Nuclear forensic science: analysis of nuclear material out of regulatory control. *Annu Rev Earth Planet Sci* 44:555–579
- Keegan E, Kristo MJ, Toole K et al (2016) nuclear forensics: scientific analysis supporting law enforcement and nuclear security investigations. *Anal Chem* 88:1496–1505. <https://doi.org/10.1021/acs.analchem.5b02915>
- Varga Z, Wallenius M, Krachler M et al (2021) Trends and perspectives in nuclear forensic science. *TrAC Trends Anal Chem* 146:116503. <https://doi.org/10.1016/j.trac.2021.116503>
- Zhang R, Nadeau K, Gautier EA et al (2021) Certification of uranium isotope amount ratios in a suite of uranium ore concentrate certified reference materials. *Geostand Geoanalytical Res n/a*. <https://doi.org/10.1111/ggr.12409>
- Toole K, Roffey P, Young E et al (2019) Evaluation of commercial forensic DNA extraction kits for decontamination and extraction of DNA from biological samples contaminated with radionuclides. *Forensic Sci Int*. <https://doi.org/10.1016/j.forsciint.2019.06.025>
- Taylor F, Higginson M, Marsden O, Schwantes J (2020) State of practice and emerging application of analytical techniques of nuclear forensic analysis: highlights from the 5th collaborative materials exercise of the nuclear forensics International Technical Working Group (ITWG). *J Radioanal Nucl Chem* 323:415–430. <https://doi.org/10.1007/s10967-019-06950-7>
- Jovanovic SV, Weber PK, Pidduck AJ et al (2020) Uncovering uranium isotopic heterogeneity of fuel pellets from the fifth collaborative materials exercise of the nuclear forensics international technical working group. *J Radioanal Nucl Chem* 326:1853–1866. <https://doi.org/10.1007/s10967-020-07470-5>
- Stebelkov V, Elantsev I, Hedberg M et al (2018) Determination of isotopic composition of uranium in the CMX-4 samples by SIMS. *J Radioanal Nucl Chem* 315:417–423. <https://doi.org/10.1007/s10967-017-5664-5>
- Park J, Kim TH, Lee C-G et al (2017) Combinatory use of time-of-flight secondary ion mass spectrometry (SIMS) and sector-field SIMS for estimating elemental and isotopic compositions of nuclear forensic samples. *J Radioanal Nucl Chem* 311:1535–1544. <https://doi.org/10.1007/s10967-016-5070-4>
- Lewis LA, Knight KB, Matzel JE et al (2015) Spatially-resolved analyses of aerodynamic fallout from a uranium-fueled nuclear test. *J Environ Radioact* 148:183–195. <https://doi.org/10.1016/j.jenvrad.2015.04.006>
- Hedberg PML, Peres P, Fernandes F, Renaud L (2015) Multiple ion counting measurement strategies by SIMS- A case study from nuclear safeguards and forensics. *J Anal At Spectrom* 30:2516–2524. <https://doi.org/10.1039/c5ja00382b>
- Krachler M, Varga Z, Nicholl A et al (2018) Spatial distribution of uranium isotopes in solid nuclear materials using laser ablation multi-collector ICP-MS. *Microchem J* 140:24–30. <https://doi.org/10.1016/j.microc.2018.03.038>
- Reilly DD, Beck CL, Buck EC et al (2020) Focused ion beam for improved spatially-resolved mass spectrometry and analysis of radioactive materials for uranium isotopic analysis. *Talanta*. <https://doi.org/10.1016/j.talanta.2020.120720>
- Van Elteren JT, Šelih VS, Šala M (2019) Insights into the selection of 2D LA-ICP-MS (multi)elemental mapping conditions. *J Anal At Spectrom* 34:1919–1931. <https://doi.org/10.1039/c9ja00166b>
- Varga Z, Wallenius M, Nicholl A, Mayer K (2020) Assessment of uranium inhomogeneity and isotope imaging for nuclear forensics. *Spectrochim Acta - Part B At Spectrosc*. <https://doi.org/10.1016/j.sab.2020.105920>

17. Certificate of Analysis Certified Reference Material CRM U010 (5mg) Uranium (U3O8) Isotopic Standard 1.0% U-235, 5 mg U, November 2020. <https://www.energy.gov/nnsa/nbl-program-office> (Accessed on 25/11/2021)
18. Certificate Standard Reference Material U-030 Uranium Isotopic Standard 3.0% U-235, 5 mg U, April 21, 1969. <https://www-s.nist.gov/srmors/certificates/archives/U-030.pdf> (Accessed on 25/11/2021)
19. Varga Z, Krachler M, Nicholl A et al (2018) Accurate measurement of uranium isotope ratios in solid samples by laser ablation multi-collector inductively coupled plasma mass spectrometry. *J Anal At Spectrom* 33:1076–1080. <https://doi.org/10.1039/c8ja0006a>
20. Hedberg PML, Peres P, Fernandes F et al (2018) Latest improvements in isotopic uranium particle analysis by large geometry-secondary ion mass spectrometry for nuclear safeguards purposes. *J Vac Sci Technol B Nanotechnol Microelectron.* <https://doi.org/10.1116/1.5016943>
21. Tanner M, Günther D (2009) Short transient signals, a challenge for inductively coupled plasma mass spectrometry, a review. *Anal Chim Acta* 633:19–28. <https://doi.org/10.1016/j.aca.2008.11.041>

Publisher's Note Springer Nature remains neutral with regard to jurisdictional claims in published maps and institutional affiliations.